JACS
JOURNAL OF THE AMERICAN CHEMICAL SOCIETY
Article
pubs.acs.org/JACS

Hydrogen-Bonded Cyclic Water Clusters Nucleated on an Oxide Surface

Coleman X. Kronawitter,[†] Christoph Riplinger,[‡] Xiaobo He,[†] Percy Zahl,[∥] Emily A. Carter,[‡,§] Peter Sutter,[∥] and Bruce E. Koel*[,†]

[†]Department of Chemical and Biological Engineering, Princeton University, Princeton, New Jersey 08544, United States
[‡]Department of Mechanical and Aerospace Engineering, Program in Applied and Computational Mathematics, Princeton University, Princeton, New Jersey 08544, United States
[§]Andlinger Center for Energy and the Environment, Princeton University, Princeton, New Jersey 08544, United States
[∥]Center for Functional Nanomaterials, Brookhaven National Laboratory, Upton, New York 11973, United States

Supporting Information

ABSTRACT: We report the observation and molecular-scale scanning probe electronic structure (dI/dV) mapping of hydrogen-bonded cyclic water clusters nucleated on an oxide surface. The measurements are made on a new type of cyclic water cluster that is characterized by simultaneous and cooperative bonding interactions among molecules as well as with both metal and oxygen sites of an oxide surface. Density functional theory + U + D calculations confirm the stability of these clusters and are used to discuss other potential water-oxide bonding scenarios. The calculations show that the spatial distributions of electronic states in the system are similar in character to those of the lowest unoccupied molecular orbitals of hydrogen-bonded water molecules. On the partially oxidized Cu(111) investigated here, experiment and theory together suggest that Cu vacancies in the growing islands of cuprous oxide inhibit water adsorption in the centers of the islands (which have reached thermodynamic equilibrium). A stoichiometric, less stable cuprous oxide likely exists at island edges (the growth front) and selectively binds these water clusters.

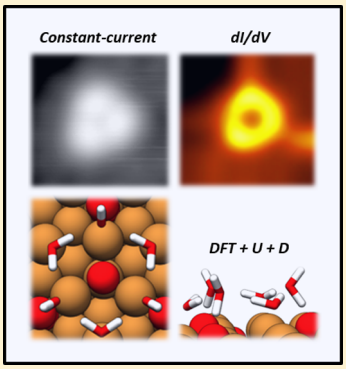

INTRODUCTION

When water interacts with a solid, an energetic competition exists between hydrogen bonding among adjacent water molecules and bonding with the surface. The outcome of this competition yields phenomena at the water−surface interface that are integral to a number of technologically critical processes: water dissociation, heterogeneous ice nucleation, wetting, as well as the development of the double layer in aqueous electrochemical systems.[1,2] At low coverage, water clusters form when lateral hydrogen bonding between water molecules is favored over individual molecules bonding to the surface (associated with wetting). Clustering is often observed on close-packed metal surfaces, such as Cu(111),[3,4] Ag(111),[4,5] and Pd(111),[6] where it is possible for highly organized structures resembling natural ice to develop (e.g., the highly stable *cyclic hexamer*). Water is less likely to cluster on pristine nonmetallic (including oxide) surfaces,[7] since these can bind water strongly and often are associated with a potential energy landscape that inhibits molecule diffusion.[2] Here using scanning probe techniques we report the first observations of a new type of hydrogen-bonded cyclic water cluster that is characterized by a simultaneous and cooperative bonding interaction with both metal and oxygen sites of an oxide surface. Detailed electronic structure measurements are performed to map the spatial and energetic distributions of electronic states associated with adsorbed water. Density functional theory + U calculations confirm the stability of these clusters and are used to discuss other potential water-oxide bonding scenarios.

The observations are made on highly defective $Cu_2O(111)$, an oxide semiconductor whose aqueous electrochemistry and photoelectrochemistry are of interest for enabling solar fuel synthesis in energy conversion devices.[8,9] The observation of room temperature-stable cyclic water clusters on an oxide surface is relevant to this application, since our mechanistic understanding of electron transfer across oxide-H_2O interfaces involves the electric double layer and therefore the structure of surface-bound H_2O molecules.[10] Our calculations differentiate between strongly bound clusters consisting of H_2O molecules coordinatively bonded to metal sites and those clusters of H_2O molecules only hydrogen-bonded to oxygen sites, a distinction important for reactions whose activation energies are tied to the displacement of surface-bound H_2O.

Clusters of water molecules are prototypical systems for understanding the interactions that govern hydrogen bonding.[11,12] The bonding rules governing cluster formation increase in complexity when nucleation occurs on a surface.[1] In the context of water adsorption on metals, the competition between the ability of H_2O molecules to bond to a substrate and to accept H bonds originates from the bonds' common

Received: June 14, 2014
Published: September 2, 2014

   dx.doi.org/10.1021/ja5056214 | J. Am. Chem. Soc. 2014, 136, 13283−13288

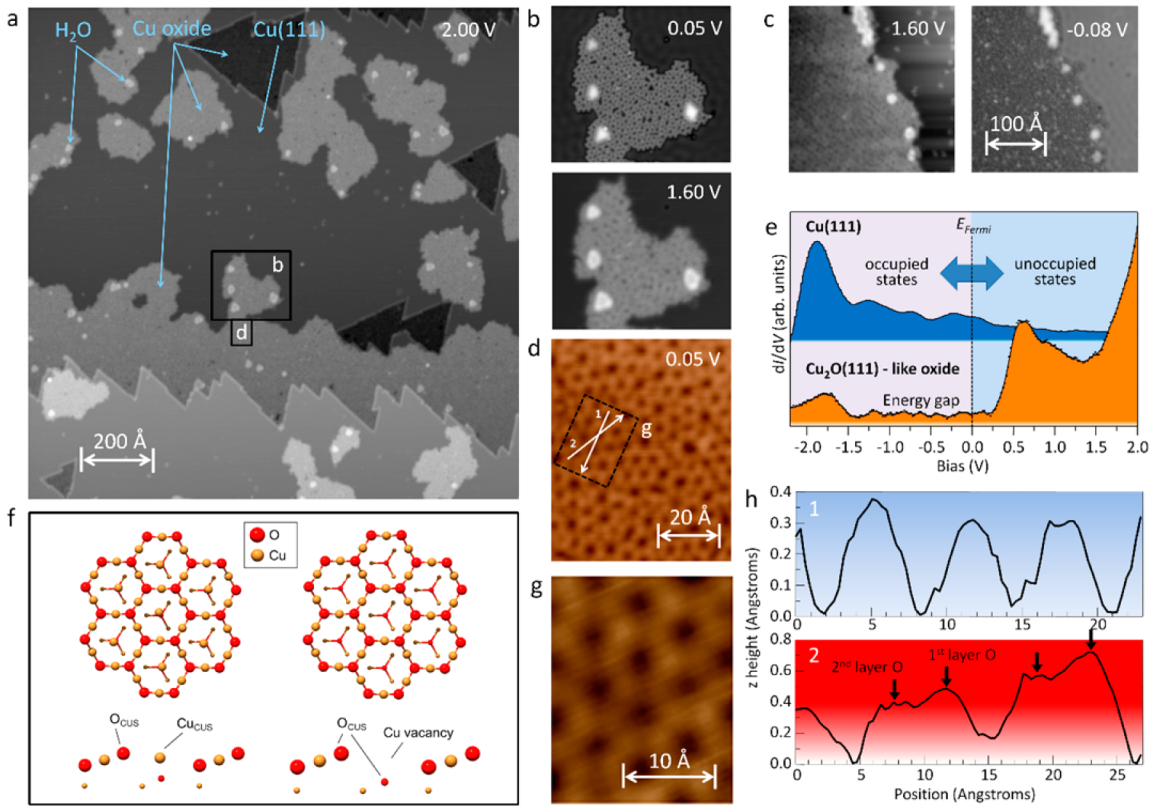

Figure 1. Unoccupied-state constant-current STM images of oxidized Cu(111) at 5 K. (a) Overview showing Cu(111) terraces, oxidized Cu(111), and water clusters (highest contrast); 2.00 V, 0.20 nA. (b) Magnified view of the highlighted region (227 Å image width) in (a), containing four water clusters, at two different bias conditions; 1.60 and 0.05 V, 0.20 nA. (c) Oxide region prepared by oxygen dosing near 450 K, followed by water adsorption; 1.60 and −0.08 V, 0.20 nA (d) Magnified view of an oxide region from a; 0.05 V, 0.20 nA. (e) *dI*/*dV* spectra taken on Cu(111) and the oxide region of a 300-K-oxidized sample. (f) Schematic of the stoichiometric $Cu_2O(111)$ surface (left), and that with Cu vacancies (right). Lower layer atoms are shown smaller for illustrative purposes only. (g) Magnified image of an ordered region of the oxide; 0.05 V, 0.20 nA. (h) Line scans showing the height variation along the arrows in d.

involvement of the nonbonding oxygen-localized $1b_1$ molecular orbital, the highest occupied molecular orbital (HOMO) of water.[3] The presence of surface oxygen atoms on metal oxides provides additional opportunities for H bonding. Consequently, less is known about the nature of water bonding on oxides. Water is observed to cluster and/or dissociate in 2D networks on MgO(100),[13] form interesting dynamic bonding networks on ZnO(10$\bar{1}$0),[14] form weakly ordered overlayers with 2 × 2 symmetry on TiO_2(101),[15] and form ordered ice structures on alumina[16] and silica.[17] We present here the first report on molecular-scale observation and electronic structure mapping of individual, room temperature-stable, cyclic water clusters on any oxide surface.

RESULTS AND DISCUSSION

Figure 1a shows a Cu(111) single crystal observed by scanning tunneling microscopy (STM) at 5 K after room temperature (300 K) oxidation and subsequent water adsorption at 20 K, followed by heating to 300 K. The oxidation of Cu(111) in these conditions is well documented,[18−20] and is characterized by the formation of three distinct oxide domains: triangles appearing as dark depressions, islands of oxide that nucleate on Cu(111) terraces, and oxide regions that grow from the edges of Cu(111) terraces. After H_2O adsorption, water clusters are observable on Cu(111) as well as on all oxidized domains on the surfaces. Heating to 300 K induces desorption of the majority of water from Cu(111), with the remaining water existing as clusters with a ring-like topography near the edges of oxide regions (highest contrast clusters in Figure 1a). Four H_2O clusters from the specified region are shown magnified in Figure 1b. STM images associated with the adsorption of water on this surface at lower temperatures, as well as additional images of the four clusters at alternate bias conditions, are shown in the Supporting Information.[21] The nucleation of water clusters is not unique to room-temperature oxidized Cu(111). Figure 1c shows STM images of clusters nucleated on the edges of oxide regions prepared by dosing O_2 with the sample held near 450 K. A small percentage of clusters are exceptions and are observed toward the center of oxide domains.

The oxide overlayer on Cu(111) prepared in these conditions can be described as a highly defective $Cu_2O(111)$ surface. Figure 1d−h provides details on the copper oxide formed here. The oxide possesses a large, open honeycomb-like structure, with ordered domains a few nanometers in size. It is clear that on longer length scales the oxide possesses numerous vacancies as well as highly strained regions with irregular bond lengths.

The assignments of atomic positions in the (111) projection of Cu_2O are shown in Figure 1f. The surface is comprised of hexamers with first- and second-layer oxygen atoms on the vertices and copper atoms between vertices. We consider two cases: the stoichiometric surface and the surface containing Cu vacancies. The two models shown are both in agreement with

dx.doi.org/10.1021/ja5056214 | J. Am. Chem. Soc. 2014, 136, 13283−13288

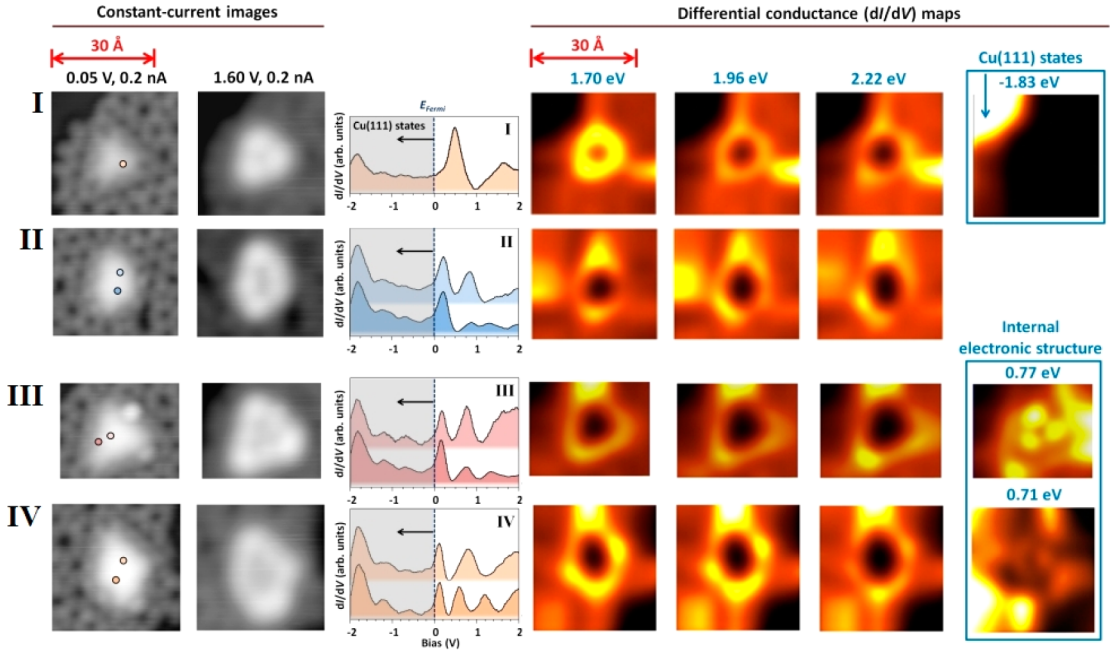

Figure 2. Left: Constant-current STM images of four water clusters (T = 5 K). Center: Differential conductance measurements on the four water clusters obtained at locations indicated by colored dots. Right: Spatially resolved differential conductance (dI/dV) maps of the four clusters at the indicated energies. Higher contrast corresponds to a greater dI/dV signal at that position.

available STM and low-energy electron diffraction data from the literature. They differ by the coordinatively unsaturated Cu in the first layer.[22] On the basis of observations and thermodynamic arguments presented later in this article, it seems likely a single structural model is insufficient to fully describe the growing oxide on Cu(111).[21] Figure 1g is an STM image of the oxide (whose borders are defined in Figure 1d), in which the hexamers are resolved, showing in our interpretation protrusions corresponding to oxygen atoms.

Measurements of the differential tunneling conductance dI/dV were used to assess the local density of states as a function of energy[23] (see eq S5, Supporting Information). Figure 1e shows representative dI/dV spectra of the Cu(111) surface and of the copper oxide surface. The copper oxide spectrum indicates the presence of a bandgap of about 1.8 eV, lower than that of bulk Cu_2O, which has been previously observed in oxide overlayers on Cu(111).[24] In Cu_2O, the valence and conduction band extrema are derived predominantly from hybridized Cu 3*d*, O 2*p*, and Cu 4*s* states.[25,26]

Figure 1a–c shows that water clusters are positioned preferentially near the edges of copper oxide islands. The four clusters in Figure 1b are shown magnified in the left-hand side of Figure 2 (numbered **I** through **IV**, top to bottom). The image of cluster **I**, when recorded at +1.60 V, resolves three protrusions configured in the vertex positions of an approximately equilateral triangle. The distance between the centers of the spots is measured to be ca. 8.4 Å. This configuration is very similar to those identified in numerous previous STM studies of H_2O adsorption[4−6] and is representative of a cyclic H_2O cluster, which to date has only been reported to have been imaged on close-packed hexagonal metal surfaces. Clusters **II** and **IV** lack the 3-fold symmetry found in **I**. The large cluster **III** has 3-fold symmetry, and again consists of a triangular structure with bright protrusions on the vertex positions, but is physically much larger than the cyclic cluster **I**.

A rich and comprehensive literature exists describing the nature of cyclic water clusters on close-packed metal surfaces.[3−5] The structure of the cluster depends on the nature of the substrate: reactive surfaces are usually associated with molecules at the same height (planar clusters), while less reactive surfaces are associated with molecules at two distinct heights (buckled).[3] For partially dissociated water clusters on hexagonal crystalline substrates, a planar configuration can also exist: the lowest energy configuration of H_2O−OH clusters on Ru(0001) maintains all oxygen atoms in the same plane.[27] On Ag(111) a water cluster with 3-fold symmetry has been ascribed to the cyclic hexamer.[5] On this surface, the visualization in STM measurements of three of six total molecules in the water hexamer has been rationalized in terms of the orbital anisotropy associated with adsorbed water clusters. In the naturally occurring form of ice, I_h, there exists a hexagonal unit cell. In any given layer, water molecules are H-bonded into hexagonal rings, with alternating molecules raised or lowered relative to the central plane (buckled structure).[1]

Scanning probe techniques allow the visualization of substrate and adsorbate electronic structure by monitoring the current from electron tunneling events to and from the system at specified energies (see eq S4, Supporting Information). Differential conductance (dI/dV) mapping in scanning tunneling spectroscopy (STS) permits in addition the evaluation of the local density of states (LDOS $\propto dI/dV$)[23] with high spatial resolution, such that the spatial distribution of specific features in the electronic structure of adsorbed molecules can be assessed. That is, molecules and molecular clusters can be visualized according to, for example, the occupancy of electronic states at specified energies with respect to the Fermi energy. As is the convention in the scanning probe literature, throughout this article we consider dI/dV measurements as direct local probes of the electronic structure.

Representative local dI/dV spectra on water clusters at locations indicated in the adjacent constant-current STM

dx.doi.org/10.1021/ja5056214 | J. Am. Chem. Soc. 2014, 136, 13283−13288

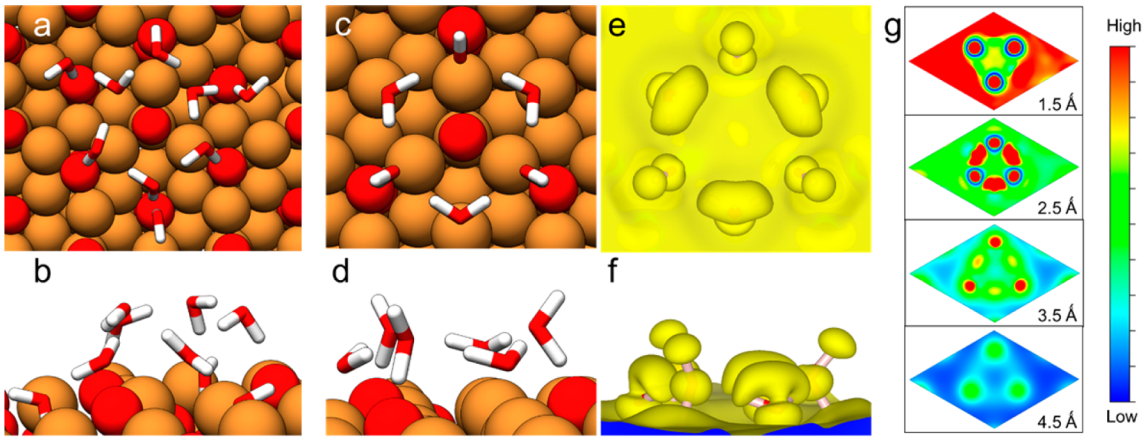

Figure 3. Atomic model of the water hexamer on the $Cu_2O(111)$ surface with Cu vacancies (a,b) and of the water hexamer on the stoichiometric $Cu_2O(111)$ surface (c,d), top view (a,c) and side view (b,d). a and b depict nine molecules, three of which lie underneath a water hexamer, filling vacancies in the surface structure. (e–g) Isosurface of charge densities (0.0002 e/Å^3) integrated over 1 eV of the unoccupied bands close to E_{Fermi}, for the model in c,d. Top view (e), side view (f) and two-dimensional cuts through the system (g) parallel to the Cu_2O (111) surface (height of the cut given in reference to a plane through the three unsaturated Cu atoms). The scale depicts the electron density.

images are shown in the center of Figure 2. The spectra show characteristic peaks (i.e., electronic states) whose energies do not change with position within the same cluster, although the intensities can change or vanish. This likely indicates that the associated electronic states are partially delocalized throughout the molecule–substrate system probed here.

The spatial distributions of electronic states in the water clusters **I**–**IV** in Figure 1b, and in the adjacent oxide and metal regions, were mapped by recording spectra across encompassing rectangular grids (see Supporting Information[21]). The resulting dI/dV maps are shown on the right-hand side of Figure 2 (additional maps are provided in the Supporting Information[21]). The intensity distribution (color scale) is normalized separately within each image. These maps show a composite of the distributions of unoccupied states (at the specified energies above the Fermi level) in the water cluster, the oxide, and the metallic substrate, since each of the individual LDOS is involved in the overall electron tunneling event from the tip to the metal substrate. However, only the water clusters were associated with pronounced peaks in the spectra, whereas Cu(111) and the copper oxide were associated with spectra that varied relatively smoothly with energy. At negative bias, a condition associated with electrons flowing from the sample to the tip, the density of states of the underlying metal substrate contributes strongly to the signal. This observation is made clear in the dI/dV map on the top right-hand side of Figure 2. Here, at −1.83 V, the occupied states of the Cu(111) substrate show high intensity in the region where the clean metal is imaged.

Above E_{Fermi}, ring-like distributions of unoccupied states are observed, consistent with the expected density of states associated with the water molecules (discussed in detail below). Recently it was shown by experiment and theory that the energies are not representative of those of the lowest unoccupied states of free H_2O molecules, and instead correspond to those of H_2O molecules coupled to the continuum of states in the STM tip.[7] An exception exists at low energies (ca. < 0.5 eV) above the Fermi level, at which a large conductance channel localized to the centers of clusters is observed (shown and discussed in the Supporting Information[21]).

For clusters **III** and **IV** at intermediate energies (between about 0.5 and 1 eV) a distribution of states highlighting an *internal structure* of the clusters is observed (far right-hand side of Figure 2). This is most clear for the case of cluster **III**, where at 0.77 eV three lobes are observed *inside* the larger structure with triangular shape. The physical separation between these lobes is close to that of the protrusions in the constant-current STM image of cluster **I**. For cluster **IV**, although the structure is less resolved, internal molecules also appear to be probed at 0.71 V (bottom right-hand side).

On the basis of these observations, we conclude that a variety of water cluster sizes and configurations are stable on this oxide surface. The observation in larger clusters (**III** and **IV**) of an internal electronic structure resembling a smaller cyclic cluster suggests this is most likely a larger assembly of molecules. Its triangular shape closely resembles that of the water nonamer, previously observed on Ag(111) surfaces.[4] In the model developed for clusters on closed packed metal surfaces, larger clusters grow by further "hydration" of the initial cyclic hexamer. The ability to further resolve here the internal structure of the nonamer is a consequence of the sensitivity of the dI/dV measurement to lateral variations in the local electronic structure signatures of the molecules. The combination of constant-current or topography STM images and dI/dV maps provides high resolution and a more comprehensive description of the molecular cluster.

Next, as a first approximation of the system studied experimentally, we use calculations employing density functional theory + U. All calculations were performed within the Vienna Ab-Initio Simulation Package.[28] DFT + U + D theory[29] with Perdew–Burke–Ernzerhof (PBE)[30,31] exchange-correlation and semiempirical dispersion corrections[32] was used to optimize the structures of the slab + water, the bare slab, and an isolated water molecule, and to calculate free energies. We used an ab initio U–J value of 3.6 eV recently determined from electrostatically embedded Hartree–Fock calculations[33] using the method of Mosey et al.[34] Our approach, in the context of the available literature on this system, is discussed in detail in the Supporting Information.[21] We model water clusters on two $Cu_2O(111)$ surfaces and calculate their stability. We considered the water hexamer, which is the constituent basis of the larger cyclic clusters.[4] The placement of the hexamer on the

dx.doi.org/10.1021/ja5056214 | J. Am. Chem. Soc. 2014, 136, 13283–13288

underlying substrate is largely dictated by the limited spatial extent of intermolecular hydrogen bonding.

The theoretically most stable surfaces in these conditions are the ideal stoichiometric surface and the surface possessing copper vacancies (see Figure 1f).[35] The stoichiometric surface contains coordinatively unsaturated copper (Cu_{CUS}) and oxygen (O_{CUS}) ions; the surface with Cu vacancies contains only coordinatively unsaturated oxygen ions. Water adsorption favorably occurs via these unsaturated ions; water hydrogens can form hydrogen bonds to O_{CUS} and water oxygens can coordinate to Cu_{CUS}. Several adsorbed water molecules can stabilize each other in a cooperative manner via water−water hydrogen bonds, as has been observed for water hexamers on metal surfaces.[4] We tested different initial configurations for smaller water configurations (monomers to tetramers) and found that the most favorable configurations have alternating hydrogen-bonded and datively bonded waters, which additionally exhibit water−water hydrogen bonds. On the basis of these most stable configurations, we constructed the initial configurations for optimization of the water clusters presented here. Our DFT + U + D results show that under UHV conditions and at low temperatures (20 K), both surfaces bind the water clusters. Increasing the temperature to 300 K leads to desorption of the water cluster on the surface with Cu vacancies, whereas on the stoichiometric surface the adsorbed water hexamer remains stable (see Supporting Information[21]).

What is the reason for this difference in stability? To answer this question we examine the bonding on both surfaces. On the stoichiometric $Cu_2O(111)$ surface we find a template of alternating O_{CUS} and Cu_{CUS} that are in close proximity (3.1 to 4.1 Å) to each other. As can be seen in Figure 3c,d this template leads to a water hexamer with three of the water molecules forming coordination bonds to Cu_{CUS} and the remaining three waters forming hydrogen bonds to O_{CUS}. The protons from the coordinated waters act as hydrogen bond donors to the adjacent waters. Concomitantly, the water molecules that are hydrogen-bonded to O_{CUS} accept these hydrogen bonds, with one of their own hydrogens involved in bonding neither to the cluster nor to the oxide surface. The surface with Cu vacancies on the other hand is associated with a less favorable template (see Figure 3a,b). The surface layer oxygen ions O_{CUS} are too far apart (about 6 Å), and the unsaturated oxygen ions in the subsurface are not oriented favorably for any exposed oxygen ions to form a template for a water cluster. A favorable template can be constructed by first binding water molecules to subsurface oxygen ions, thus filling the Cu vacancy sites (see Supporting Information).[21] The subsurface-bound water and the surface layer oxygen ions have interatomic distances of 3.1 to 3.9 Å, which can then act as a template for a water cluster. A water hexamer can form on top of such a template. The six water molecules bind alternately to surface oxygen ions and subsurface-bound water and are further stabilized by two hydrogen bonds, each water acting both as hydrogen bond donor and acceptor. This yields in total nine bound water molecules per surface: three water molecules to fill up the vacancies plus the water hexamer. This ice-like bonding is not strong enough to facilitate water cluster adsorption at room temperature and under UHV conditions, though we do find it is sufficient to bind the cluster at higher pressure or lower temperature (see Supporting Information[21]).

The STM measurements taken after heating to room temperature (Figures 1a,b and 2) show water clusters preferentially adsorb on the edges of oxide regions. We now address this in the context of our DFT + U + D results. Our calculations show that under these experimental conditions, water clusters are expected to exist only on the stoichiometric surface, and not on the surface possessing Cu vacancies. We believe the water clusters are acting as a probe for the underlying surface structure. Thus, on the basis of this premise we suggest that the centers of the oxide islands possess Cu vacancies (unresolved in our images) and the edges are the stoichiometric oxide. We can now combine the experimental observation with the theoretical findings on the $Cu_2O(111)$ surface stability: the surface with Cu vacancies is predicted to be more stable than the stoichiometric surface.[35] This suggests that the Cu_2O in the center of the islands has reached a stable thermodynamic equilibrium state, while that on the edges of the islands is at an earlier stage of the surface oxidation process and possesses a higher surface energy. It is reasonable to assume that the observed small percentage of clusters adsorbed near the centers of oxide domains (Figure 1a) are probing localized regions that have yet to reach the thermodynamic equilibrium state, perhaps because of the unique history of the oxide growth at that position. This explanation is consistent with the experimental conditions; after oxygen dosing, the crystal was rapidly cooled to extreme low temperatures. This is also in-line with the general notion that surfaces with higher energy are more reactive. This explanation for the observation of preferential cluster nucleation near the edges of oxide regions does not consider the influence of localized electronic effects associated with the edge, for example, the presence of a dipole moment through the Smoluchowski effect.[36] This is justified by our observation that the adsorption does not occur *directly at* the edge, as would be expected for reactivity driven by the Smoluchowski effect, typically found on step edges of clean metal surfaces.

For comparison with dI/dV maps in Figure 2, we calculated isosurfaces of charge densities in the water clusters, integrated over 1 eV of the unoccupied bands close to the Fermi energy. The resultant real-space images are shown in Figure 3e,f. The charge densities closely resemble the lowest unoccupied molecular orbitals of water.[7] The orbital lobes throughout the cluster are arranged in a triangular cyclic structure, qualitatively similar to what is observed in the dI/dV maps associated with cluster **I** in Figure 2. This is made clear in the two-dimensional cuts through the system in Figure 3g. The isosurfaces of the three hydrogen-bonded waters form local protrusions within the combined isosurface of the water hexamer, spatially extending outward about 0.8 Å. The orbital anisotropy evident in the isosurface plots explains the origin of our imaging three of six total water molecules in cluster **I**: the intensity of the measured tunneling current relates in part to the orbital overlap corresponding to the relative geometric position of the tip atoms and the sample atoms, i.e., to the convolution of the LDOS in the tip and the sample[21] (eq S4, Supporting Information).

■ CONCLUSIONS

The cyclic water clusters observed and characterized here extend our understanding of the nature of hydrogen-bonded water clusters generally, as well as of the cooperative bonding of groups of water molecules to substrates. The characteristics of interfacial bonding discussed are expected to be applicable to other metal oxide surfaces as well, as site-specific bonding of water, as well as the existence of hydrogen-bonded clusters, have been observed spectroscopically on oxides.[37,38] Vibrational

dx.doi.org/10.1021/ja5056214 | J. Am. Chem. Soc. 2014, 136, 13283−13288

spectroscopies can play an important role in further investigating these bonding characteristics, although the influence of local variations in the substrate structure discussed here suggests that careful experimental considerations are required. Additional future work should emphasize the implications of local water cluster structure on the behavior of water at higher coverages (length scales) and perhaps multiple time scales, as characteristics in these domains have been shown to be influenced by the competition between water−metal and water−water interactions.[39]

The thermodynamic accessibility of these structures heteronucleated on oxide surfaces has implications for numerous applications, including aqueous (photo)-electrochemical systems for energy conversion, where the structure and orientation of water molecules and the energetic distribution of their electronic states can determine interfacial charge transfer efficiency. Indeed in aqueous electrochemical systems, ice-like water vibrational signatures have been measured in situ.[40]

Here we can consider as a topical example heterogeneous water dissociation. Water dissociation occurs in general by excitation of the molecule into a repulsive electronic state.[41] It has been demonstrated that one such state is characterized by an excited electron occupying an antibonding orbital that was previously unoccupied.[41] The general technique of measurement and calculation of the spatial distributions of unoccupied states within water structures presented here is therefore additionally relevant to the atomic-scale design of water reduction catalysts,[42] which are known to involve site-specific electron transfer mechanisms.

■ ASSOCIATED CONTENT

Supporting Information

Experimental and computational details, STM images at alternate temperatures and tunneling conditions, and additional STS maps. This material is available free of charge via the Internet at http://pubs.acs.org.

■ AUTHOR INFORMATION

Corresponding Author

bkoel@princeton.edu

Author Contributions

The manuscript was written through contributions of all authors. All authors have given approval to the final version of the manuscript.

Notes

The authors declare no competing financial interest.

■ ACKNOWLEDGMENTS

C.X.K. and B.E.K. acknowledge support from the Grand Challenges Program at Princeton University. C.R. and E.A.C. acknowledge financial support from the Air Force Office of Scientific Research and supercomputing resources from the DoD High Performance Computing Modernization Program. Research carried out in part at the Center for Functional Nanomaterials, Brookhaven National Laboratory, which is supported by the U.S. Department of Energy, Office of Basic Energy Sciences, under Contract No. DE-AC02-98CH10886.

■ REFERENCES

(1) Thiel, P. A.; Madey, T. E. *Surf. Sci. Rep.* **1987**, *7*, 211.
(2) Henderson, M. A. *Surf. Sci. Rep.* **2002**, *46*, 1.
(3) Carrasco, J.; Hodgson, A.; Michaelides, A. *Nat. Mater.* **2012**, *11*, 667.
(4) Michaelides, A.; Morgenstern, K. *Nat. Mater.* **2007**, *6*, 597.
(5) Morgenstern, K.; Nieminen, J. *Phys. Rev. Lett.* **2002**, *88*, 066102.
(6) Mitsui, T.; Rose, M. K.; Fomin, E.; Ogletree, D. F.; Salmeron, M. *Science* **2002**, *297*, 1850.
(7) Guo, J.; Meng, X. Z.; Chen, J.; Peng, J. B.; Sheng, J. M.; Li, X. Z.; Xu, L. M.; Shi, J. R.; Wang, E. G.; Jiang, Y. *Nat. Mater.* **2014**, *13*, 184.
(8) Kuhl, K. P.; Cave, E. R.; Abram, D. N.; Jaramillo, T. F. *Energy Environ. Sci.* **2012**, *5*, 7050.
(9) Paracchino, A.; Laporte, V.; Sivula, K.; Gratzel, M.; Thimsen, E. *Nat. Mater.* **2011**, *10*, 456.
(10) Aitken, D. G.; Cox, P. A.; Egdell, R. G.; Hill, M. D.; Sach, I. *Vacuum* **1983**, *33*, 753.
(11) Keutsch, F. N.; Saykally, R. J. *Proc. Natl. Acad. Sci. U. S. A.* **2001**, *98*, 10533.
(12) Xantheas, S. S. *Chem. Phys.* **2000**, *258*, 225.
(13) Verdaguer, A.; Sacha, G. M.; Bluhm, H.; Salmeron, M. *Chem. Rev.* **2006**, *106*, 1478.
(14) Dulub, O.; Meyer, B.; Diebold, U. *Phys. Rev. Lett.* **2005**, *95*, 136101.
(15) He, Y. B.; Tilocca, A.; Dulub, O.; Selloni, A.; Diebold, U. *Nat. Mater.* **2009**, *8*, 585.
(16) Al-Abadleh, H. A.; Grassian, V. H. *Langmuir* **2003**, *19*, 341.
(17) Kaya, S.; Weissenrieder, J.; Stacchiola, D.; Shaikhutdinov, S.; Freund, H. J. *J. Phys. Chem. C* **2007**, *111*, 759.
(18) Jensen, F.; Besenbacher, F.; Stensgaard, I. *Surf. Sci.* **1992**, *269*, 400.
(19) Jensen, F.; Besenbacher, F.; Laegsgaard, E.; Stensgaard, I. *Surf. Sci.* **1991**, *259*, L774.
(20) Yang, F.; Choi, Y.; Liu, P.; Stacchiola, D.; Hrbek, J.; Rodriguez, J. A. *J. Am. Chem. Soc.* **2011**, *133*, 11474.
(21) See Supporting Information.
(22) Önsten, A.; Gothelid, M.; Karlsson, U. O. *Surf. Sci.* **2009**, *603*, 257.
(23) Sutter, P. In *Science of Microscopy*; Hawkes, P. W., Spence, J. C. H., Eds; Springer: New York, 2007; pp 969−1024.
(24) Wiame, F.; Maurice, V.; Marcus, P. *Surf. Sci.* **2007**, *601*, 1193.
(25) Nolan, M.; Elliott, S. D. *Phys. Chem. Chem. Phys.* **2006**, *8*, 5350.
(26) Isseroff, L. Y.; Carter, E. A. *Phys. Rev. B: Condens. Matter Mater. Phys.* **2012**, *85*, 235142.
(27) Feibelman, P. J. *Science* **2002**, *295*, 99.
(28) Kresse, G.; Joubert, D. *Phys. Rev. B: Condens. Matter Mater. Phys.* **1999**, *59*, 1758.
(29) Dudarev, S. L.; Botton, G. A.; Savrasov, S. Y.; Humphreys, C. J.; Sutton, A. P. *Phys. Rev. B: Condens. Matter Mater. Phys.* **1998**, *57*, 1505.
(30) Perdew, J. P.; Burke, K.; Ernzerhof, M. *Phys. Rev. Lett.* **1996**, *77*, 3865.
(31) Perdew, J. P.; Burke, K.; Ernzerhof, M. *Phys. Rev. Lett.* **1997**, *78*, 1396.
(32) Grimme, S. *J. Comput. Chem.* **2006**, *27*, 1787.
(33) Yu, K.; Carter, E. A. *J. Chem. Phys.* **2014**, *140*, 121105.
(34) Mosey, N. J.; Liao, P.; Carter, E. A. *J. Chem. Phys.* **2008**, *129*, 014103.
(35) Bendavid, L. I.; Carter, E. A. *J. Phys. Chem. B* **2013**, *117*, 15750.
(36) Smoluchowski, R. *Phys. Rev.* **1941**, *60*, 661.
(37) Zwicker, G.; Jacobi, K. *Surf. Sci.* **1983**, *131*, 179.
(38) Takeuchi, M.; Martra, G.; Coluccia, S.; Anpo, M. *J. Phys. Chem. B* **2005**, *109*, 7387.
(39) Limmer, D. T.; Willard, A. P.; Madden, P.; Chandler, D. *Proc. Natl. Acad. Sci. U. S. A.* **2013**, *110*, 4200.
(40) Ataka, K.; Yotsuyanagi, T.; Osawa, M. *J. Phys. Chem.* **1996**, *100*, 10664.
(41) Morgenstern, K.; Rieder, K. H. *Chem. Phys. Lett.* **2002**, *358*, 250.
(42) Jaramillo, T. F.; Jorgensen, K. P.; Bonde, J.; Nielsen, J. H.; Horch, S.; Chorkendorff, I. *Science* **2007**, *317*, 100.